

Conducted emission investigation of infant incubator heating control mode

Khusnul Khotimah¹, Yoppy², Muhammad Imam Sudrajat^{2,3}, Vera Permatasari², Elvina Trivida², Tyas Ari Wahyu Wijanarko^{2,4}

¹Research Center for Advanced Material, National Research and Innovation Agency, Tangerang, Indonesia

²Research Center for Testing Technology and Standards, National Research and Innovation Agency, Tangerang, Indonesia

³Electrical Engineering, Mathematics and Computer Science, University of Twente, Enschede, Netherlands

⁴School of Electrical Engineering and Informatics, Bandung Institute of Technology, Bandung, Indonesia

Article Info

Article history:

Received Oct 22, 2021

Revised Jun 13, 2022

Accepted Jul 8, 2022

Keywords:

Conducted emission

Heating power system

Infant incubator

Phase angle control mode

Zero-crossing control mode

ABSTRACT

This paper investigates the effect of two different heating power control systems of infant incubators on their conducted emissions. Two infant incubators which respectively employ zero-crossing control mode and phase angle control mode are observed. The research was conducted by measuring conducted electromagnetic interference (EMI) from each infant incubator's power input. Measurements are conducted both during full power condition, while the incubator's compartment temperature is far away from the temperature setpoint, and during power chopping condition, while the compartment temperature reaches the steady-state set point. Method and limit of the measurement refer to CISPR 11. It is found that conducted emission higher than the standard CISPR 11 limit occurs during power chopping on phase angle control mode. This results from the sharp rise time of voltage delivered to the heater, around 220 ns for each chopping cycle.

This is an open access article under the [CC BY-SA](https://creativecommons.org/licenses/by-sa/4.0/) license.



Corresponding Author:

Khusnul Khotimah

Research Center for Advanced Material, National Research and Innovation Agency

Puspipstek Area, Setu, South Tangerang, Banten 15314, Indonesia

Email: khusnul.khotimah@lipi.go.id

1. INTRODUCTION

A modern infant incubator is a device with a rigid enclosure intended to keep in a baby and provided with means to control its internal environment at a temperature of 36-37 °C and relative humidity of 70% up to 75% [1]–[3]. The incubator provides a safe, clean and warm environment where temperature and humidity can be controlled by warm air inside the enclosure. In general, incubators have a transparent section for viewing the baby, an alternating current (AC)-powered heater, a fan for air circulation, a water container to control humidity, access ports for nursing care, and a control valve through which oxygen may be supplied when necessary. Incubators have numerous advantages and have been widely used, but also have some hidden disadvantages that should be considered, namely electromagnetic interference (EMI) [4]–[6]. EMI is an undesirable electromagnetic disturbance that results from the propagation of conducted or radiated electromagnetic signals [7]. Uncontrolled EMI can resonate and cause malfunctions or misreading of medical devices [8], [9]. Devices with higher EMI have more potential to trigger performance degradation [10]. Previous studies reported the robust electromagnetic energy emitted by wireless devices has been contributing to electromagnetic pollution [11] and is responsible for most vital medical device malfunctions [12].

On the other hand, the heating system in the infant incubator needs a controller to keep the compartment temperature matching the setpoint value [13], [14]. However, the switching mechanism of the

heater driver contributes the most EMI. Two controller modes regulate the amount of power delivered to the heater, namely zero-crossing control mode and phase angle control mode. Zero-crossing control mode regulates the amount of power by varying the percentage of delivered power within a set of cycles window. Meanwhile, phase angle control mode regulates power by varying delivered power within every electrical cycle. The negative influence of the infant incubator will be even greater if its harmonics level is high [15]–[17]. This source, if not properly controlled, can emit high EMI which can interfere with the reading of bioelectric signals or disturb other sensitive medical devices. In other cases, equipment such as an electrosurgery unit (ESU) or other operating devices is also potentially affected by this noise and this will be hazardous for both patient and medical devices operators. Many studies have been carried out to overcome electromagnetic interference in several areas [18]–[21].

Furthermore, the EMI can propagate by radiation through the air and by conduction mechanism through a conductive material [7], [22]. In hospitals, several propagation mechanisms of EMI can occur such as via a coupling through electrical installation, a radiative coupling, and crosstalk between noisy mains cables and data cables [10]. Many studies have discussed the magnetic field or electromagnetic radiated emission (RE) produced by incubators [6] [23], [24]. On the contrary, very few studies have investigated the electromagnetic conduction emissions (CE) produced by infant incubators.

In view of these shortcomings, this paper investigates the CE noise produced by two infant incubators with different control modes. Both infant incubators use a triode for alternating current (TRIAC) as a component to regulate the heater power. The investigation of CE is carried out during the full power and chopping conditions. The finding of this study is very important, especially for infant incubator developers who want to fulfill the electromagnetic compatibility (EMC) requirements. The method and limit of CE measurement were carried out refer to CISPR 11:2019.

2. INFANT INCUBATOR POWER HEATING

The main purpose of an infant incubator is to provide a conditioned environment inside the compartment for the newborn. The environment of the compartment is conditioned by blowing filtered ambient air through heating elements and water reservoirs. The heating element is required to maintain the temperature in the compartment in the range of setpoint temperature. The percentage of power delivered to the heating element is controlled to maintain the compartment temperature within the setpoint range, where the percentage of power depends on the temperature difference between the setpoint and that of the compartment. The average power supplied to the heating element is controlled by adjusting the connection of the power source to the heater using TRIAC.

TRIAC is a semiconductor device widely used for switching low to medium power AC to control large power load applied in electronic equipment and appliances for rectifier, inverter, frequency modulation, voltage adjustment, and contactless switch [25]. TRIAC is triggered by applying either a positive or negative small voltage to the gate to control medium-power AC. Its switching turn-on and turn-off behavior will cause changes in current and voltage in a short period [25]–[27] and generate conducted and radiated EMI [20], [28], [29]. The fast ON-OFF and OFF-ON state transition of switches causes EMI due to the high dv/dt ratios, which generate transient charge currents in inter-wire capacitances of cables, intra-winding capacitances of transformers, and p–n junctions of power diodes, as well as transient circuit-to-ground currents through parasitic capacitances [30]. Rapid transient voltage and current changes during turn-on and turn-off result in the sharp-edge transients containing most of the frequency components. The most significant contributions to the EMI spectrum are at the fundamental switching frequency and its harmonics [28]. The faster the switching the greater the content of high-frequency harmonics in the switched current and voltage waveforms [31].

3. RESEARCH METHOD

Experiments were carried out on two infant incubator samples, each of which used different control systems. The first infant incubator uses zero-crossing control mode, while the second uses phase angle control mode. The infant incubator's temperature setpoint was at 37 °C over the time of data collection. The voltage waveform applied to the heater is measured using Tektronix MDO3014 Mixed Domain Oscilloscope. The block diagram of the test can be shown in Figure 1.

The CE testing was done in the shielded chamber to see the effect of different temperature control systems on the generated electromagnetic interference. The power cable of the infant incubator was connected to the NNB 41 Schaffner line impedance stabilizing network (LISN), which was connected to the AC power line. LISN was used to measure the CE from the infant incubator precisely because it isolates the equipment under test (EUT) from unwanted interference signals on the supply mains [32]. The infant incubator was placed 0.8 m away from LISN. The distance between the EUT and the vertical ground plane is

0.4 m. Measurement was performed in the frequency range of 150 to 30 MHz using Advantest U3751 spectrum analyzer.

Method of testing and emission limits refer to CISPR 11 standard, especially on testing of conducted disturbance clause. The limit of CE that must be complied by the infant incubator specified by the CISPR 11 is shown in Figure 2. The block diagram of CE testing is shown in Figure 3. The CE testing system can take measurements in two modes: scanning mode and in-depth measurement mode. Scanning mode measures the magnitude of an input signal using peak detector in the frequency range that was set before measurement. After scanning mode is finished, suspected frequencies found during scanning mode can be processed into in-depth measurement mode using quasi-peak and average detector to obtain a more accurate emission level of respective frequencies. The in-depth measurement process takes more time than the scanning mode process does.

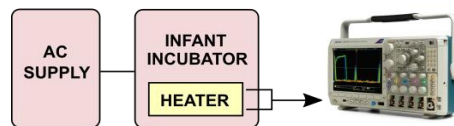


Figure 1. Block diagram of heater measurement using an oscilloscope

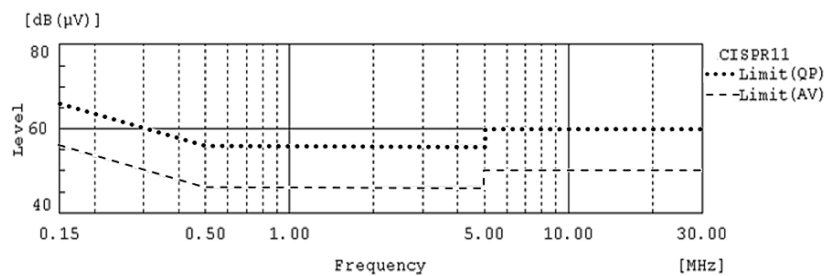


Figure 2. CE CISPR 11 standard limit [33]

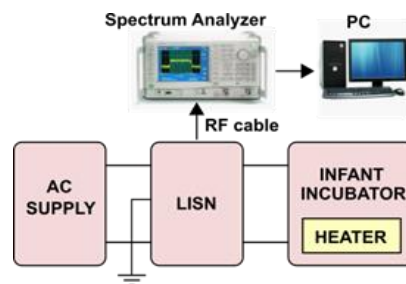


Figure 3. Block diagram of CE testing

4. RESULTS AND DISCUSSION

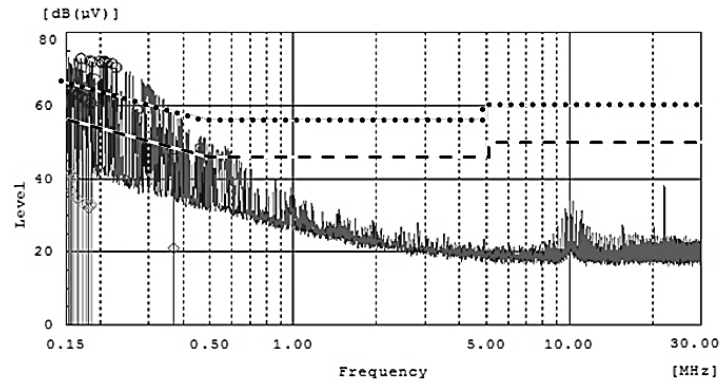
The amount of power delivered to the heater is regulated by the infant incubator's temperature controller. The amount of power delivered depends on the temperature difference between the setpoint and compartment temperature, in which the temperature sensor is placed. The wider the distance between the setpoint and the compartment's temperature, the greater the power percentage. Both control modes i.e., phase angle control mode and zero-crossing control mode are measured in full power condition and power chopping condition. Each mode produces distinctive CE profiles.

4.1. During full power

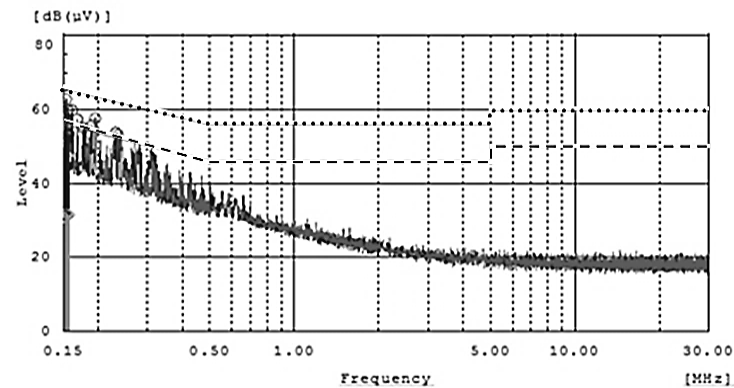
During full power conditions, the power is continuously delivered to the heater with the same magnitude over time, and there is no interruption in delivering power to the heater. It means there are no changes to the power delivered to the heater. Figure 4 shows Infant incubator with zero-crossing control

exhibits higher CE EMI than infant incubators with phase angle control during full power, as shown in Figure 4(a) for zero-crossing control mode and 4(b) for phase angle control mode.

It can be seen from Figure 4, CE emitted by the zero-crossing control mode is slightly higher than that of phase angle control mode during the full power condition. The higher CE appears in zero-crossing control mode originating from the delayed trigger which is unavoidable in the zero-crossing detector being used (MOC3041) [34]. This leads to a sharp RF current shortly after every zero-crossings, as seen in Figure 5. Figure 6 shows delay in zero-crossing trigger causes a delay in the heater turning on which results in the heater input voltage rising abruptly with a rise time of 640 ns. Figure 6 shows a closer observation of the current spike on zero-crossing during full power delayed turn-on in Figure 6(a) and turn-on rise time in Figure 6(b).



(a)



(b)

Figure 4. CE signature during full power of (a) zero-crossing control mode and (b) phase angle control mode

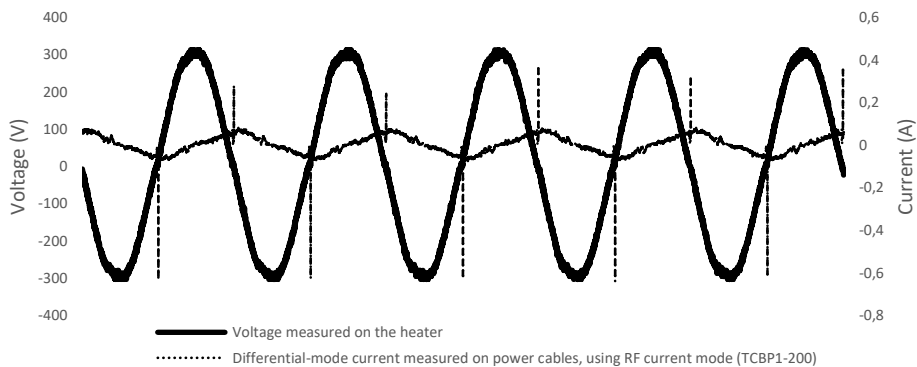


Figure 5. Current spike on zero-crossing during full power

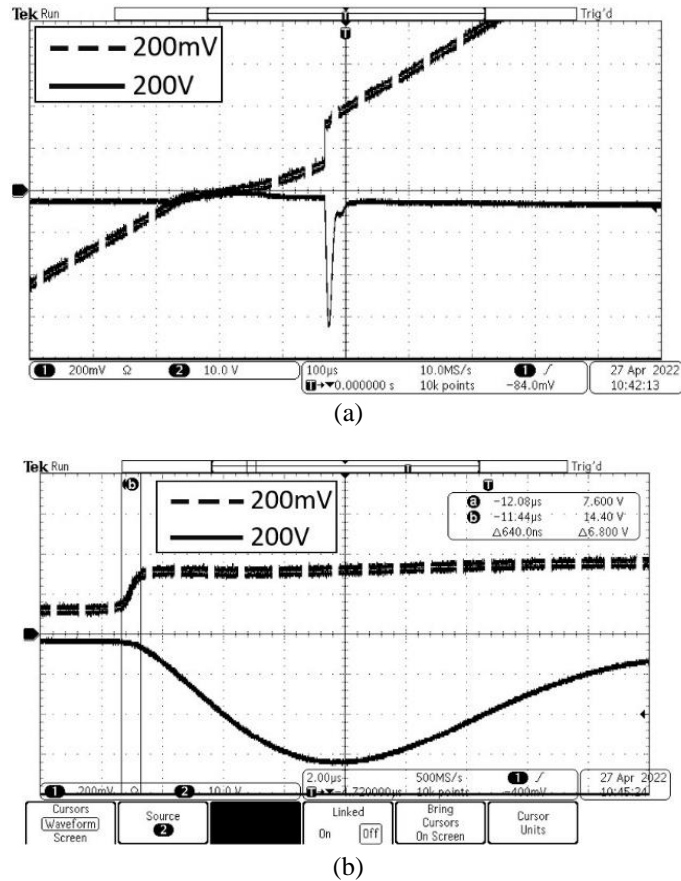


Figure 6. Closer observation of Figure 5 around zero-crossing (a) delayed turn-on and (b) measuring turn-on rise time

The number of current spikes is proportional to the percentage of power delivered to the heater. During power chopping, the number of current spikes will decrease and CE emitted will be lower. Therefore, the lowest CE will be observed when the compartment temperature reaches the setpoint, as can be seen in Figure 7(a). Meanwhile, in the phase angle control mode, this phenomenon does not occur and the voltage delivered to the heater during full power is purely sinusoidal. Figure 7 shows the CE signature during power chopping for zero-crossing control mode in Figure 7(a) and phase angle control mode in Figure 7(b). However, both CE emitted are below the limit stated in CISPR 11. This is seen after in-depth measurements were made on the suspected frequencies found in scanning mode during full power. The final result of the in-depth measurement can be seen in Tables 1 and 2. Tables 1 and 2 show the final measurement results both for phase angle control mode and zero-crossing control mode are pass for every suspected frequency. Which means that the measured value on each frequency does not exceed the limit specified in CISPR 11 as illustrated in Figure 2.

4.2. During power chopping

While the temperature of the infant incubator compartment is approaching the setpoint, the amount of power delivered to the heater is reduced by chopping the power to keep the compartment's temperature as close the set point as possible. The power chopping cycle can be done within one electrical cycle or a set of cycles. Power chopping on a set of cycles occurs on the zero-crossing control mode, as shown in Figure 8. Power chopping within one electrical cycle (20 ms) occurs on the phase angle control mode, as seen in Figure 9.

It can be seen in Figure 8 that the alternation between interrupted and uninterrupted voltage always started at the beginning of the electrical cycle. This situation causes less distortion in the voltage waveform. As a consequence, the CE values will be lower and decrease as the number of cycles being turned on is fewer. Figure 8(a) shows the peak measurement of zero-crossing control mode infant incubator during power chopping, which is comparable to that of during full power as shown in Figure 4(a). However, the final measurement with quasi-peak and average detector shows that the CE levels of power chopping are lower by

5-6 dB compared to those of full power. This is shown in Table 3. It can be seen that the peak CE noise is below the 4 MHz frequency range, which can be interpreted as noise interference caused by the on/off switching speed behavior. This CE profile is consistent with Wan *et al.* [25].

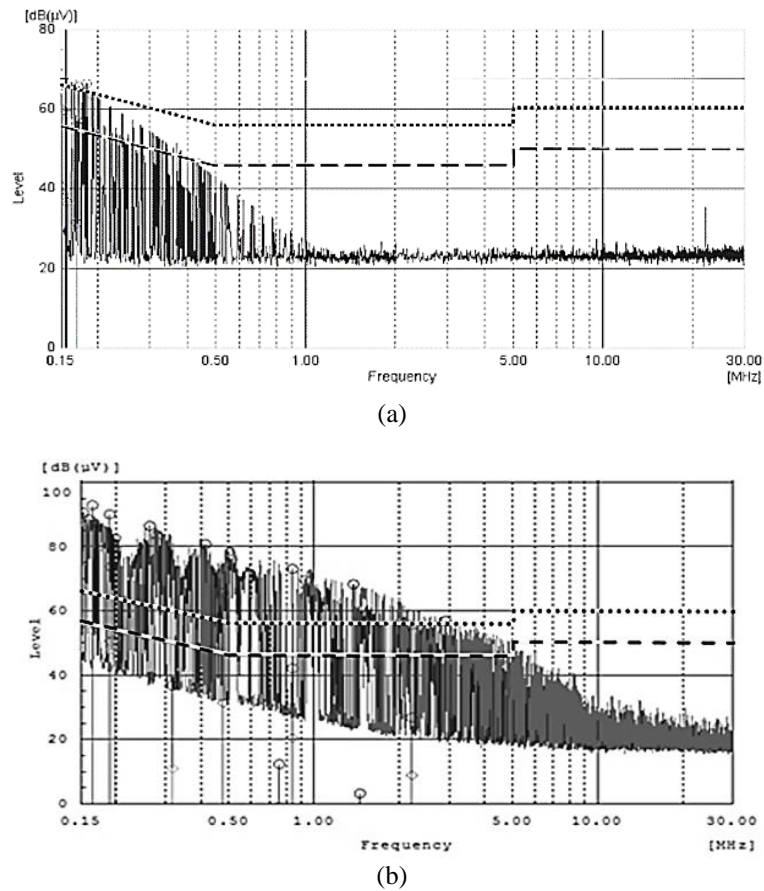


Figure 7. CE signature during power chopping of (a) zero-crossing control mode and (b) phase angle control mode

Table 1. Final data list of phase angle control mode during full power

Freq MHz	Line Phase	Level	Level	Limit	Limit	Margin	Margin	Result
		dB(uV) QP	dB(uV) AV	dB(uV) QP	dB(uV) AV	dB	dB	
0.1572	L1	53.5	31.5	65.6	55.6	12.1	24.1	Pass
0.1559	L1	53.2	31.7	65.7	55.7	12.5	24.1	Pass
0.152	L1	51.0	30.5	65.9	55.9	14.9	25.5	Pass
0.1535	L1	52.2	31.8	65.8	55.8	13.6	24.0	Pass
0.1518	L1	50.6	30.5	65.9	55.9	15.3	25.4	Pass
0.1521	L1	51.2	30.9	65.9	55.9	14.7	25.0	Pass
0.1556	L1	53.1	31.6	65.7	55.7	12.6	24.1	Pass
0.1531	N	52.1	32.0	65.8	55.8	13.7	23.8	Pass
0.1529	N	52.0	32.0	65.8	55.8	13.8	23.8	Pass
0.1555	N	52.8	31.5	65.7	55.7	12.9	24.3	Pass

It can be seen in Figure 9 that power chopping in the phase angle control mode during power chopping is started within the electrical cycle. As an effect, the heater voltage and current rise abruptly from zero to certain values, depending on the phase at the moment voltage are applied. The rise time, defined as the time required for the voltage to increase from 10% to 90%, is typically around 220 ns, as shown in Figure 10. Those sharp rising edges are known to have high-frequency contents that eventually propagate through the power cable and are measured as CE. A comparison of Figures 4(b) and 8(b) shows that the CE of the phase angle control mode during power chopping is much higher than those during full power.

Table 2. Final data list of zero-crossing control mode during full power

Freq MHz	Line Phase	Level	Level	Limit	Limit	Margin	Margin	Result
		dB(uV) QP	dB(uV) AV	dB(uV) QP	dB(uV) AV	dB QP	dB AV	
0.1561	L1	64.7	41.6	65.7	55.7	1.1	14.1	Pass
0.1856	L1	60.9	32.9	64.2	54.2	3.3	21.3	Pass
0.1778	L1	61.8	33.1	64.6	54.6	2.8	21.5	Pass
0.160	L1	64.0	40.6	65.5	55.5	1.5	14.9	Pass
0.1612	L1	63.8	40.5	65.4	55.4	1.6	15.0	Pass
0.1855	L1	60.7	32.5	64.2	54.2	3.5	21.7	Pass
0.1668	L1	63.0	34.4	65.1	55.1	2.1	20.7	Pass
0.155	L1	64.5	41.5	65.7	55.7	1.2	14.2	Pass
0.172	L1	62.3	33.5	64.9	54.9	2.7	21.4	Pass
0.1648	L1	63.1	34.5	65.2	55.2	2.1	20.7	Pass
0.154	N	63.8	41.0	65.8	55.8	2.0	14.9	Pass
0.1572	N	63.3	36.8	65.6	55.6	2.3	18.8	Pass
0.1814	N	60.3	31.9	64.4	54.4	4.1	22.5	Pass
0.3675	N	45.5	21.0	58.6	48.6	13.2	27.6	Pass

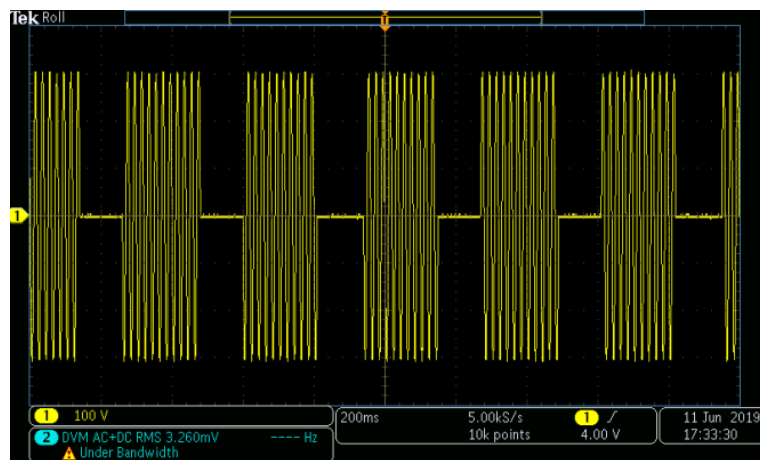


Figure 8. Voltage waveform applied to the heater on zero-crossing control mode during power chopping

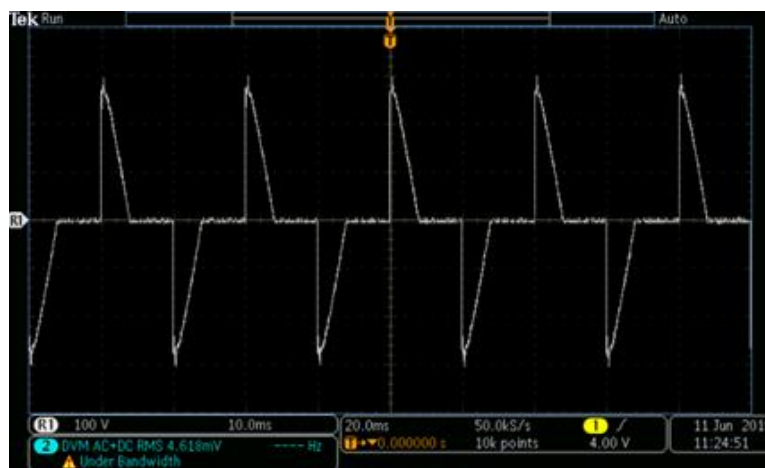


Figure 9. Voltage waveform applied to the heater on phase angle control mode during power chopping

The final result of in-depth measurement during power chopping for zero-crossing control mode and phase angle control mode is shown in Tables 3 and 4, respectively. It can be seen clearly that several frequencies of phase angle control mode during power chopping are higher than the limit stated in CISPR 11. It means that infant incubators with phase angle control mode will emit high CE value that can cause them not to comply with requirements stated in IEC 60601-1, IEC 60601-1-2, IEC 60601-2-19, and CISPR 11.

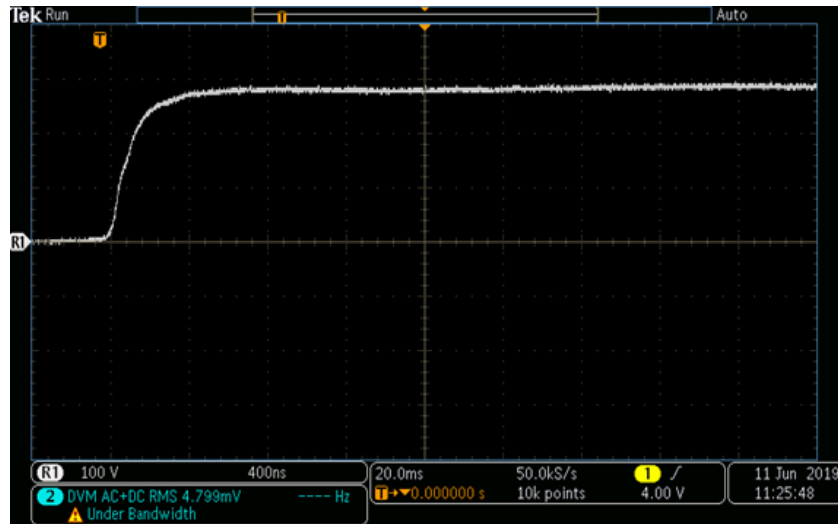


Figure 10. The rising edge of power chopping in Figure 9

Table 3. Final data list of zero-crossing control mode during power chopping

Freq MHz	Line Phase	Level dB(uV) QP	Level dB(uV) AV	Limit dB(uV) QP	Limit dB(uV) AV	Margin dB QP	Margin dB AV	Result
0.1703	N	46.9	21.2	64.9	54.9	7.7	23.4	Pass
0.1572	N	48.5	26.6	65.6	55.6	6.8	18.7	Pass
0.1520	N	49.4	27.5	65.9	55.9	6.2	18.1	Pass
0.1517	N	49.3	30.3	65.9	55.9	6.3	15.3	Pass

Table 4. Final data list of phase angle control mode during power chopping

Freq MHz	Line Phase	Level dB(uV) QP	Level dB(uV) AV	Limit dB(uV) QP	Limit dB(uV) AV	Margin dB QP	Margin dB AV	Result
0.1650	N	92.9	53.9	65.2	55.2	-27.7	1.3	Fail
0.1898	N	90.0	50.6	64.0	54.0	-26.0	3.5	Fail
0.4763	N	65.7	31.3	56.4	46.4	-9.3	15.1	Fail
0.8378	N	42.1	20.4	56.0	46.0	13.9	25.6	Pass
2.2068	N	26.8	8.8	56.0	46.0	29.2	37.2	Pass
4.8088	N	-8.6	-8.8	56.0	46.0	64.6	54.8	Pass
0.1981	L1	82.6	51.4	63.7	53.7	-18.9	2.3	Fail
0.1925	L1	73.7	48.0	63.9	53.9	-9.8	5.9	Fail
0.3161	L1	36.7	11.0	59.8	49.8	23.1	38.9	Pass
0.7534	L1	12.3	-0.6	56.0	46.0	43.7	46.6	Pass
1.4521	L1	3.2	-7.4	56.0	46.0	52.8	53.4	Pass
2.8956	L1	-6.4	-8.9	56.0	46.0	62.4	54.9	Pass

5. CONCLUSION

This study aimed to investigate the CE spectrum of two different temperature control mechanisms on infant incubators during full-power and power-chopping conditions. It was found that during full-power conditions the zero-crossing control exhibited higher CE as a result of a delay in zero-crossing detection than that of phase angle control. Nevertheless, in-depth measurements showed that the CE of both controls was below the CISPR 11 limits.

On the other hand, more concerning results were found in the power-chopping condition of the phase angle control mode. The experiment confirmed that this mode resulted in CE higher than the standard limit stated in CISPR 11 during power chopping. Power chopping occurs when infant incubator's compartment temperature is around the setpoint, which is the ideal condition for the baby placed inside. Hence, for a significant portion of time the incubator will work in power chopping mode during its operation. Other electronic devices that are connected to the same power network will get exposed to a high level of CE, which can lead to performance degradation. Unlike the phase angle control, power chopping by the zero-crossing control did not produce limit-exceeding CE. Although sharp voltage edges are unavoidable around zero-crossings, the level of CE is lower and proportional to the number of turn-on cycles.

ACKNOWLEDGEMENTS

The authors gratefully acknowledge National Research and Innovation Agency (BRIN), Republic of Indonesia for financially supporting the research activities.

REFERENCES

- [1] Z. A. Nisha and F. Elahi, "Low cost neonatal incubator with smart control system," *8th International Conference on Software, Knowledge, Information Management & Applications (SKIMA)*, 2014, doi: 10.13140/2.1.4591.5201.
- [2] N. P. Reddy, G. Mathur, and S. I. Hariharan, "Toward a fuzzy logic control of the infant incubator," *Annals of Biomedical Engineering*, vol. 37, no. 10, pp. 2146–2152, Oct. 2009, doi: 10.1007/s10439-009-9754-6.
- [3] K. R. Olson and A. C. Caldwell, "Designing an early stage prototype using readily available material for a neonatal incubator for poor settings," in *Annual International Conference of the IEEE Engineering in Medicine and Biology*, Aug. 2010, pp. 1100–1103., doi: 10.1109/IEMBS.2010.5627347.
- [4] R. Antonucci, A. Porcella, and V. Fanos, "The infant incubator in the neonatal intensive care unit: unresolved issues and future developments," *Journal of Perinatal Medicine*, vol. 37, no. 6, pp. 587–598, Jan. 2009, doi: 10.1515/JPM.2009.109.
- [5] J. El Hadj Ali, E. Feki, M. A. Zermani, C. de Prada, and A. Mami, "Incubator system identification of humidity and temperature: comparison between two identification environments," in *9th International Renewable Energy Congress (IREC)*, Mar. 2018, pp. 1–6., doi: 10.1109/IREC.2018.8362529.
- [6] C. V. Bellieni, V. Nardi, G. Buonocore, S. Di Fabio, I. Pinto, and A. Verrotti, "Electromagnetic fields in neonatal incubators: the reasons for an alert," *The Journal of Maternal-Fetal and Neonatal Medicine*, vol. 32, no. 4, pp. 695–699, Feb. 2019, doi: 10.1080/14767058.2017.1390559.
- [7] C. R. Paul, *Introduction to electromagnetic compatibility*, 2nd ed. Hoboken, NJ, USA: John Wiley & Sons, Inc., 2005, doi: 10.1002/0471758159.
- [8] O. Lauer, M. Riederer, N. Karoui, R. Vahldieck, E. Keller, and J. Frohlich, "Characterization of the electromagnetic environment in a hospital," in *Asia-Pacific Symposium on Electromagnetic Compatibility and 19th International Zurich Symposium on Electromagnetic Compatibility*, May 2008, pp. 474–477, doi: 10.1109/APEMC.2008.4559915.
- [9] J. F. Coll, J. J. Choquehuana, J. Chilo, and P. Stenumgaard, "Statistical characterization of the electromagnetic environment in a hospital," in *2010 Asia-Pacific International Symposium on Electromagnetic Compatibility*, Apr. 2010, pp. 289–292, doi: 10.1109/APEMC.2010.5475847.
- [10] C. Luca and A. Salceanu, "Study upon electromagnetic interferences inside an intensive care unit," in *International Conference and Exposition on Electrical and Power Engineering*, Oct. 2012, pp. 535–540, doi: 10.1109/ICEPE.2012.6463878.
- [11] Y. A. Garces-Gomez, V. Henao-Céspedes, and L. F. Diaz-Cadavid, "Electromagnetic pollution maps as a resource for assessing the risk of emissions from mobile communications antennas," *International Journal of Electrical and Computer Engineering (IJECE)*, vol. 10, no. 4, pp. 4244–4251, Aug. 2020, doi: 10.11591/ijece.v10i4.pp4244-4251.
- [12] M. Y. I. Maria, W. Z. W. I. Yazmin, Z. Zainoz, A. A. Azlan, and A. Tarmizi, "A review on electromagnetic band gap application in medical devices," *Materials Today: Proceedings*, vol. 16, pp. 2047–2051, 2019, doi: 10.1016/j.matpr.2019.06.090.
- [13] D. A. R. Wati, "Design of type-2 fuzzy logic controller for air heater temperature control," in *2015 on Science and Technology (TICST)*, Nov. 2015, pp. 360–365, doi: 10.1109/TICST.2015.7369386.
- [14] K. Khotimah, M. I. Sudrajat, and S. Wahyu Hidayat, "Infant incubator temperature controlling and monitoring system by mobile phone based on Arduino," in *2019 International Seminar on Research of Information Technology and Intelligent Systems (ISRITI)*, Dec. 2019, pp. 494–498, doi: 10.1109/ISRITI48646.2019.9034646.
- [15] M. J. Ghorbani, S. Atashpar, A. Mehrafruz, and H. Mokhtari, "Nonlinear loads effect on harmonic distortion and losses of distribution networks," *26th International Power System Conference*, 2015, doi: 10.13140/2.1.5047.3288.
- [16] K. Kulkarni and V. J. Shetty, "Power quality issues in healthcare centre," *International Journal of Current Engineering and Technology*, vol. 4, no. 3, pp. 3–6, 2014.
- [17] M. E. Balci and M. H. Hocaoglu, "Effects of source voltage harmonic distortion on power factor compensation in TRIAC controlled ac chopper circuits," in *2005 International Conference on Power Electronics and Drives Systems*, 2005, vol. 2, pp. 1199–1204., doi: 10.1109/PEDS.2005.1619870.
- [18] Z. M'barki, K. S. Rhazi, and Y. Mejdoub, "A proposal of structure and control overcoming conducted electromagnetic interference in a buck converter," *International Journal of Power Electronics and Drive Systems (IJPEDS)*, vol. 13, no. 1, pp. 380–389, Mar. 2022, doi: 10.11591/ijpeds.v13.i1.pp380-389.
- [19] V. Sreekumar and S. A. "A review of the EMI mitigation techniques in power converters," *SSRN Electronic Journal*, pp. 1–5, 2019, doi: 10.2139/ssrn.3448322.
- [20] U. M. Yuvaraj, A. Alagarsamy, A. K. Loganathan, and S. Thavassy, "Conducted emission study in space vector modulated voltage source inverter," *International Journal of Power Electronics and Drive Systems (IJPEDS)*, vol. 13, no. 2, pp. 988–997, Jun. 2022, doi: 10.11591/ijpeds.v13.i2.pp988-997.
- [21] M. Y. Hariyawan, R. Hidayat, and E. Firmansyah, "The effects of spread-spectrum techniques in mitigating conducted EMI to LED luminance," *International Journal of Electrical and Computer Engineering (IJECE)*, vol. 6, no. 3, pp. 1332–1343, Jun. 2016, doi: 10.11591/ijece.v6i3.9528.
- [22] M. El Hajji, H. Mahmoudi, and M. Labbadi, "The electromagnetic interference caused by high voltage power lines along the electrical railway equipment," *International Journal of Electrical and Computer Engineering*, vol. 10, no. 5, pp. 4581–4591, Oct. 2020, doi: 10.11591/ijece.v10i5.pp4581-4591.
- [23] I. Calvente, A. Vázquez-Pérez, M. F. Fernández, M. I. Núñez, and A. Muñoz-Hoyos, "Radiofrequency exposure in the neonatal medium care unit," *Environmental Research*, vol. 152, pp. 66–72, Jan. 2017, doi: 10.1016/j.envres.2016.09.019.
- [24] C. V. Bellieni *et al.*, "Electromagnetic fields produced by incubators influence heart rate variability in newborns," *Archives of Disease in Childhood - Fetal and Neonatal Edition*, vol. 93, no. 4, pp. 298–301, Apr. 2007, doi: 10.1136/adc.2007.132738.
- [25] J. Wan, Z. Zeng, and M. Huang, "EMI impact by the TRIAC zero crossing detection trigger," in *IEEE 5th International Symposium on Electromagnetic Compatibility (EMC)*, Oct. 2017, pp. 1–5., doi: 10.1109/EMC-B.2017.8260374.
- [26] C. F. Bearer, "Electromagnetic fields and infant incubators," *Archives of Environmental Health: An International Journal*, vol. 49, no. 5, pp. 352–354, Oct. 1994, doi: 10.1080/00039896.1994.9954986.
- [27] G. Çabuk and S. Kilinç, "Reducing electromagnetic interferences in flyback AC-DC converters based on the frequency modulation technique," *Turkish Journal of Electrical Engineering and Computer Sciences*, vol. 20, no. 1, pp. 71–86, 2012, doi:

- 10.3906/elk-1007-577.
- [28] J. Balcells *et al.*, “Frequency modulation techniques for EMI reduction in SMPS,” in *European Conference on Power Electronics and Applications*, 2005, vol. 2005, pp. 8–10, doi: 10.1109/EPE.2005.219198.
- [29] J. D. Kagerbauer and T. M. Jahns, “Development of an active dv/dt control algorithm for reducing inverter conducted EMI with minimal impact on switching losses,” in *IEEE Power Electronics Specialists Conference*, 2007, pp. 894–900, doi: 10.1109/PESC.2007.4342107.
- [30] A. M. Trzynadlowski, “EMI effects of power converters,” in *Power Electronics Handbook*, Elsevier, 2011, pp. 1229–1245, doi: 10.1016/B978-0-12-382036-5.00042-2.
- [31] T. Williams, “Digital and analogue circuit design,” in *EMC for Product Designers*, Elsevier, 2017, pp. 330–386, doi: 10.1016/B978-0-08-101016-7.50013-4.
- [32] T. Williams, “RF emissions measurements,” in *EMC for Product Designers*, Elsevier, 2017, pp. 139–191, doi: 10.1016/B978-0-08-101016-7.50007-9.
- [33] “CISPR 11 Edition 6.2 2019-01: Industrial, scientific and medical equipment - Radio-frequency disturbance characteristics-Limits and methods of measurement.” International Electrotechnical Commission, 2019.
- [34] “Application note AN-3004,” ON Semiconductor. <https://www.onsemi.jp/pub/collateral/an-3004jp.pdf> (accessed Apr. 28, 2022).

BIOGRAPHIES OF AUTHORS



Khusnul Khotimah    received a bachelor's degree in Engineering Physics Department from Universitas Gadjah Mada in 2004. She received a master's degree from Electrical engineering Universitas Indonesia in 2014. Currently, she is a researcher at BRIN – the National Research and Innovation Agency Republic of Indonesia. Her research interests include instrumentation, electrical-electronics testing technology, and low dimensional materials. She can be contacted at email: khus002@brin.go.id.



Yoppy    received a B.Eng. degree from the Electrical Engineering Department of Brawijaya University, Indonesia in 2009. He is with BRIN – the National Research and Innovation Agency Republic of Indonesia (formerly LIPI – Indonesian Institute of Sciences) since 2010. In 2010-2012 he was involved in the electromedical testing laboratory. He received the M.Sc. in Embedded Systems from the University of Twente, the Netherlands in 2014. From 2014 until now he is a member of the Applied Electromagnetics research group, BRIN. He can be contacted at email: yoppy.chia@gmail.com.



Muhammad Imam Sudrajat    received a B.Sc. degree in Engineering Physics from Gadjah Mada University, Indonesia, in 2006 and an M.Sc. degree in Biomedical Engineering from Universitas Indonesia, Indonesia, in 2016. He has worked with BRIN – the National Research and Innovation Agency Republic of Indonesia (formerly LIPI – Indonesian Institute of Sciences) since 2008. Currently, he is a Ph.D. student at Power Electronics and Electromagnetic Compatibility at the University of Twente, Enschede, The Netherlands. He can be contacted at email: m.i.sudrajat@utwente.nl.



Vera Permatasari    received Bachelor of Applied Science in Midwifery, Medical Faculty of Padjadjaran University, Bandung in 2011 and Master degree in Biomedical Science, Medical Faculty of Sriwijaya University, Palembang in 2017. Her current research is in the field of biomedical and medical device. She can be contacted at email: vera004@brin.go.id.



Elvina Trivida     received Bachelor degree in Physics from Padjadjaran University, Indonesia in 2013 and Master degree in Engineering Physics from Bandung Institute of Technology, Indonesia in 2016. Currently, she is a researcher at BRIN – the National Research and Innovation Agency Republic of Indonesia. Her research interests include electronic materials and electromagnetic applications. She can be contacted at email: elvi004@brin.go.id.



Tyas Ari Wahyu Wijanarko     received Bachelor Degree in Physics from Universitas Gadjah Mada, Indonesia in 2016. Currently, he is a Graduate Student at School of Electrical Engineering and Informatics, Bandung Institute of Technology, Bandung, Indonesia. His research interests include electromagnetic measurements and applications. He can be contacted at email: tyasariwahyu@gmail.com.